Title

Radial storage efficiency for CO2 injection: Quantifying effectiveness of local flow control methods

Journal

Greenhouse Gases Science and Technology, 11(4)

ISSN

2152-3878

Author

Oldenburg, Curtis M

Publication Date

2021-08-01

DOI

10.1002/ghg.2080

Peer reviewed

Published in Greenhouse Gases: Science and Technology, 22 June 2021
https://doi.org/10.1002/ghg.2080

Radial Storage Efficiency for CO_2 Injection: Quantifying Effectiveness of Local Flow Control Methods

Curtis M. Oldenburg
Energy Geosciences Division
Lawrence Berkeley National Laboratory
Berkeley, CA 94720

Abstract
Basin-scale geologic carbon sequestration will require hundreds of injection wells, each of which has costs related to property rights and regulatory requirements that correlate with the areal size of the carbon dioxide plume. These surface-footprint-related issues motivate maximizing storage efficiency radially away from each well. Radial storage efficiency (RSE) is defined here as the ratio of the volumetrically weighted carbon dioxide free-phase saturation within a given radius away from the injection well to the available pore space within that same radius. Maximizing RSE effectively minimizes the radial extent of the CO_2 plume. Optimizing RSE around individual wells requires local flow control injection strategies that can increase the uniformity of the filling of pore space around the well over the entire length of the perforated injection interval despite differences in local formation transmissivity. The goal of uniform filling of the storage reservoir starting from the well outward is to maximize carbon dioxide sweep and trapping locally outward from the well in all of the layers of the storage region before buoyancy forces predominate and drive carbon dioxide upward where it will spread laterally under lower-permeability layers. Example simulations of carbon dioxide injection into a layered storage system with and without local flow control are presented to show the advantage of uniformly filling all layers and how RSE can be used to quantify storage efficiency for the two different injection approaches.

Introduction
Basin-scale geologic carbon sequestration (GCS) (100 million tonnes of CO_2 or more per year) will require hundreds of individual carbon dioxide (CO_2) injection wells at numerous industrial-scale GCS project sites spread out over hundreds to thousands of square kilometers within a sedimentary basin. After decades of injection, pressure rise in the storage region will likely be the main factor limiting capacity within basins, especially if storage reservoirs behave more like closed as opposed to open hydrologic systems [1, 2, 3]. But in the early years of basin-scale GCS, maximizing pore-space-filling efficiency at individual wells will be critical to minimizing free-phase CO_2 footprint. Footprint minimization is important for reducing project costs because it minimizes the area of real estate under which the operator needs to acquire surface access and/or pore-space-filling/mineral rights, and it can reduce the likelihood of CO_2 encountering abandoned wells which could leak and/or are in need of remediation thereby facilitating the permitting process.

One way to maximize local pore-space-filling efficiency during fluid injection is to make use of local flow control methods, referred to as intelligent or smart completions in the oil and gas industry [4]. For the purposes of this paper, the various existing intelligent/smart completion approaches will not be detailed but will instead be referred to as local flow control. Regardless of whether the approach involves active/passive valves or dual/multiple completions, the goal of local flow control approaches is to achieve independent flow-rate control along different intervals in the injection well. The goal is to adapt the injection flow rate and/or pressure locally along the injection interval to the effective transmissivity of each reservoir layer. These approaches apply to both vertical, deviated, and horizontal wells. Although such approaches have been described for use in CO_2-EOR [5], they have not yet been widely discussed for GCS. Yet the potential benefits of local flow control methods for GCS are obvious given the large buoyancy driving forces and formation heterogeneity that prevent efficient reservoir sweep, along with the urgent need for widely implementing large-scale GCS for greenhouse gas mitigation purposes. The idea for GCS is that local flow control will allow CO_2 to be injected more uniformly into the pore space around the well so that more of the reservoir is swept by CO_2 as pressure and buoyancy cause flow outward and upward from the well into the storage reservoir volume. For GCS without brine extraction to control the CO_2 plume [6], the only practical controls on CO_2 migration are those implemented at and near the injection well. This is because depending on properties of the formation, its native fluids, and the CO_2 injection rate, after a certain distance of CO_2 flow away from the well, buoyancy forces become the main driving force and CO_2 tends to flow upward as controlled by formation layering and vertical permeability [7, 8].

The purpose of this paper is to present a new approach for quantifying radial storage efficiency (RSE), and to emphasize the challenge and benefits of improving CO_2 storage efficiency in the face of heterogeneity in the storage formation. This work is intended to motivate operators and reservoir engineers to apply and/or advance the technology of local flow control for applications in the growing GCS field. Use of flow control methods on a reservoir-specific basis may allow improved RSE and thereby lower the costs of siting and permitting of projects through decreased free-phase CO_2 plume sizes during both the injection and post-injection periods.

Storage Efficiency

Prior Work

The various measures of storage efficiency that have been proposed are all essentially ratios of the volume of CO_2 injected for storage to the total volume available for CO_2 storage [8]. In equations developed to estimate storage capacity, the storage efficiency can be thought of as an overall multiplier of reservoir pore-space volume that combines thefactors that tend to prevent CO_2 from filling all of the available pore space. Early investigators (van der Meer 1995; Doughty et al. (2001))[9, 10] recognized that this overall multiplier is the product of individual terms that reduce reservoir-filling efficiency (e.g., effects of phase mobility and capillary effects, buoyancy, heterogeneity, residual fluid saturation, and strength of aquifer water drive. This multiplier was further described and given the name capacity coefficient by Bachu et al. (2007)[11]. Analytical solutions developed by Nordbotten et al. (2005)[12] demonstrated the strong effects of buoyancy in preventing efficient filling of nominally horizontal reservoirs.

Mathematically for an idealized radial injection geometry, Okwen et al. [13] and Ringrose [14] defined C_c as the ratio of the total amount (mass converted to volume) of CO_2 injected to the volume of a cylinder of radius r_{max} equal to the radius of the maximum extent of the free-phase plume:

$$Cc = \left[\frac{Q\,t}{\phi\, H\, \pi\, r_{\max}^2} \right] \tag{1}$$

where Q is volumetric injection rate, t is time (t), and ϕ, H, and r_{max} are porosity, storage layer thickness, and maximum radius (radial extent) of the CO_2 plume, respectively, There is broad agreement from both the earliest work on storage efficiency [9, 10] and later work by Kopp et al. (2009b), Brennan et al. (2010), and Ringrose (2018) [15, 16, 17] that the value of the capacity coefficient (C_c) is in the single digits by volume percent.

Doughty et al. (2003) [18] and Okwen et al. (2010) [13] realized that storage volume can be considered a dynamic quantity and therefore storage efficiency can be considered to evolve as the radius of the plume footprint grows.

By the definition of C_c in Eq. 1, the storage efficiency decreases as r_{max} increases, all other things being equal. Using this approach, Okwen et al. (2010) [13] were able to quantify the loss of efficiency that occurs as CO_2 buoyantly overrides denser brine and spreads out in a thin layer underneath the base of the lower-most cap rock. Numerical simulation work by Kumar and Bryant (2008) [19] recognized the importance of buoyancy forces in reducing the efficient filling of the reservoir and looked into ways of increasing storage efficiency in the face of strong buoyancy flow. Given that there are costs associated with large plume footprints, operators of GCS sites will want to strive to keep plume radius as small as possible by maximizing storage efficiency around wells.

Extending the Capacity Coefficient Concept

To build on the prior concepts developed in [18, 13, 14], note that the radius term defining storage volume (e.g., in the denominator of Eq. 1) does not have to be the CO_2 free-phase plume extent, but can instead be considered to be any arbitrary distance (r) from the injection well, e.g., the distance to the property line of the project site, or to the property line of the pore-space owner, or to the spill point of the storage reservoir structure, etc. This way of thinking leads to defining storage efficiency based on the fraction filled by CO_2 of a cylindrical storage volume with any arbitrary radius (r) for use in the denominator of storage efficiency equations. By this approach, the most efficient storage would occur if the operator could fill to maximum capacity all of the pore space contained within a cylinder of height H and radius r.

Considering this radial flow geometry and with the objective of maximizing radial storage efficiency, it makes sense to also reconsider the numerator in Eq. 1 to recognize variation in pore-filling efficiency outward in the radial direction, and longitudinally along the well.

Published in Greenhouse Gases: Science and Technology, 22 June 2021
https://doi.org/10.1002/ghg.2080

Specifically, one can extend previous measures of storage efficiency such as that illustrated in Figure 1a and described by Eq. 1 by redefining the numerator to use a volumetrically weighted pore occupancy (that may vary with radius away from the well) rather than total injected volume. As illustrated in Figure 1b, the RSE proposed below does this and also considers spatially variable native brine residual saturation (S_{lr}) and whether residual brine saturation has been reduced by vaporization, an effect that adds nominal storage capacity in the dry-out region. Figure 1 illustrates the differences between C_c and RSE in terms of the numerator (volume of CO_2 considered) and the denominator (volume of storage reservoir considered). Note that for the case that the arbitrary $r = r_{max}$ and $S_{lr} = 0$, RSE is identical to C_c.

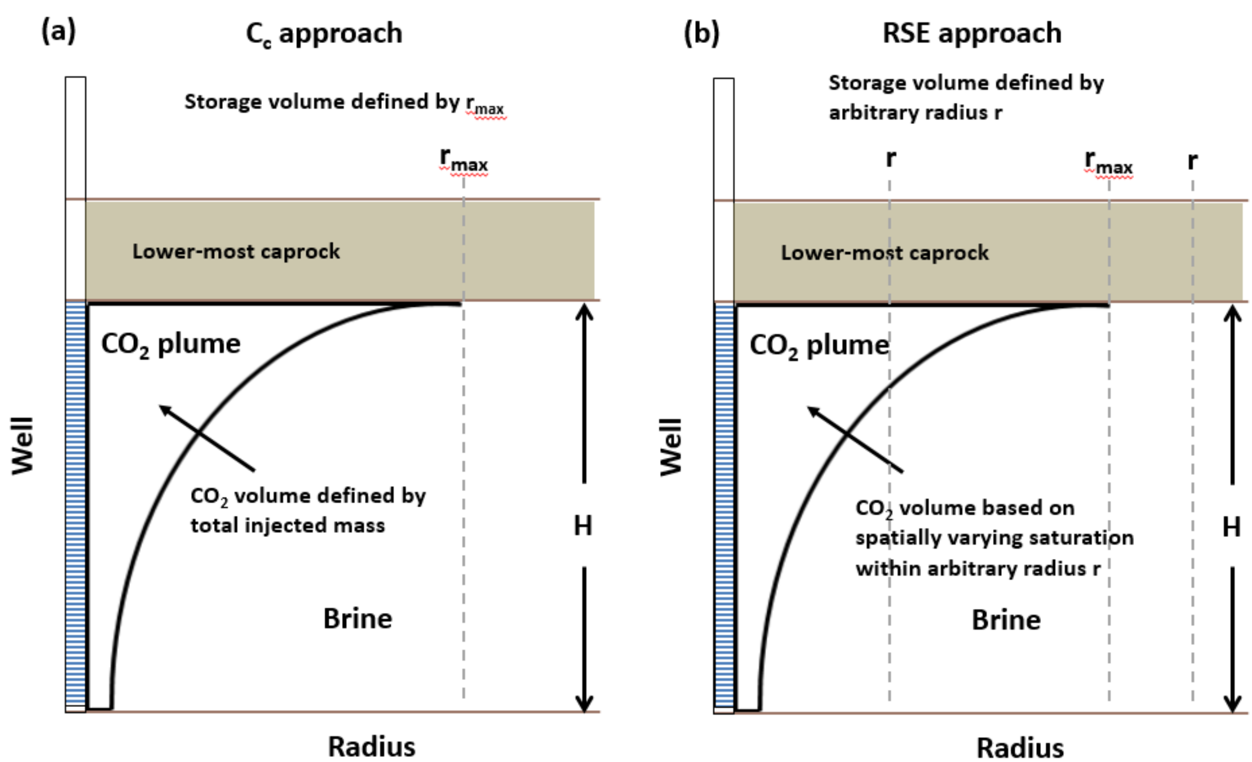

Figure 1. Illustrations of the different numerator (CO_2 volume) and denominator (radius) terms for the (a) Capacity coefficient (C_c) and (b) Radial Storage Efficiency (RSE) approaches, highlighting the differences between the two efficiency terms. Note that for the case that the arbitrary $r = r_{max}$ and $S_{lr} = 0$, RSE is identical to C_c.

Effect of a Layered Reservoir

To add a bit more realism to the discussion of storage efficiency and to motivate reservoir engineering to increase RSE, Figure 2 shows a conceptual model for radial injection into a horizontal layered system.

This figure is intended to illustrate the fact that storage regions targeted for GCS in sedimentary basins generally have layers of variable thickness and/or permeability (i.e., varying transmissivity). Because of the heterogeneous layers, standard injection approaches will result in limited injection into low-transmissivity layers while high-transmissivity layers, especially higher in the injection zone, receive the bulk of the injected CO_2 from a nominally vertical well, all other things being equal. As CO_2 flows away from the near-well region and viscous forces become subordinate to buoyancy forces within the layers, injected CO_2 tends to rise upwards which leads to relatively rapid lateral spreading in approximately horizontally layered sedimentary reservoirs. Both variable injection into the vertically heterogeneous system and buoyant rise serve to decrease radial storage efficiency because they lead to larger CO_2 plume footprints.

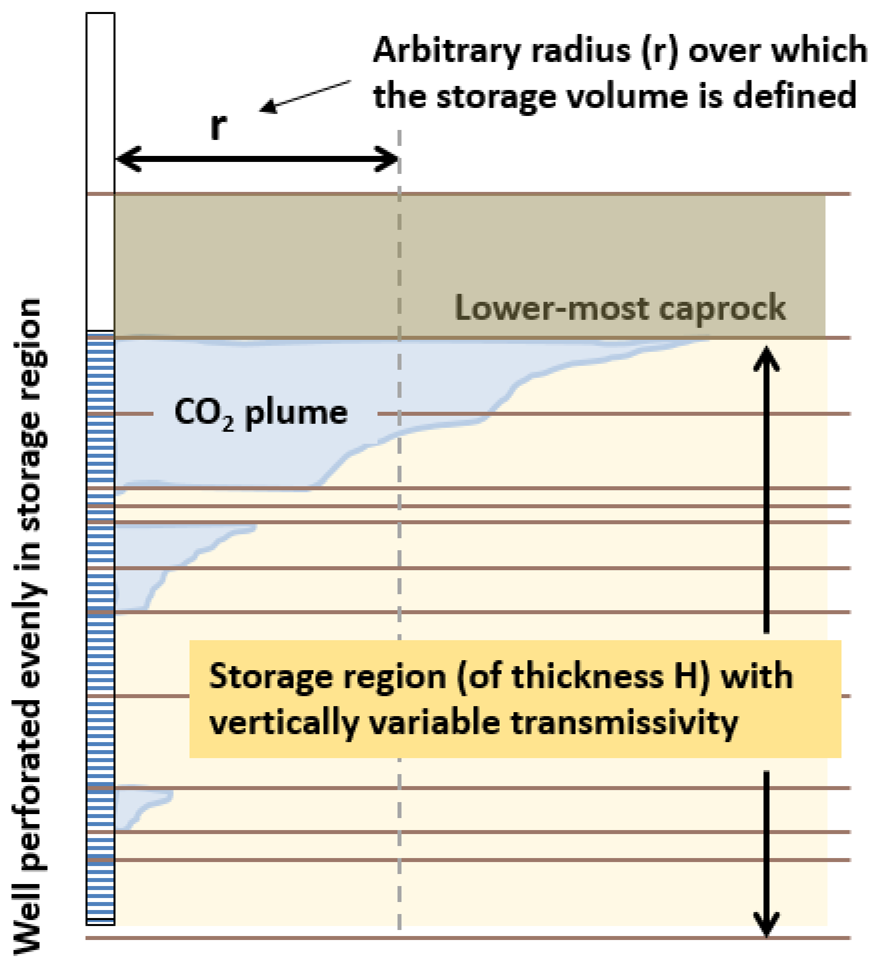

Figure 2. Sketch of a slice of an idealized radially symmetric CO_2 saturation plume following injection into a layered storage reservoir of thickness H. Low transmissivity in some layers leads to lack of injection, while the high-transmissivity layers preferentially receive injected CO_2.

Following injection and after a short period of lateral flow, buoyancy forces cause the CO_2 to flow upward within each layer.

Carbon dioxide injection into a storage reservoir through a well perforated across the injection zone can be represented as a finite line source (the well) injecting CO_2 radially outward. Because of this radial flow geometry, there will be large variations in pore-filling efficiency as a function of radius outward from the well. Specifically, the relatively large CO_2 flow velocity in the formation along the well following exit from the well perforations will diminish rapidly by purely geometric effects as the distance from the well increases. In addition, the tendency for dry (pipeline) CO_2 to vaporize native formation brine (causing dry out) that exists near the well will decrease outward away from the well as capillary and gravity forces begin to dominate [20].

Formal Definition of RSE

Following the presentation of the history of capacity efficiency and using the above concepts of CO_2 pore occupancy and arbitrary radius of storage region, we can now define RSE as the ratio of the volumetrically weighted average CO_2 saturation divided by one minus the volumetrically weighted average residual liquid (aqueous phase, or brine) saturation within the arbitrary cylindrical storage volume of radius r. Formally, the definition of RSE is

$$RSE_{CO2} = \frac{\overline{S}_{CO2}}{\left(1-\overline{S}_{lr}\right)} \qquad (2)$$

where the storage volume is defined by a cylinder of height H with arbitrary radius r around the well such that the volumetric averaging is carried out as

$$\overline{S}_{CO2} = \frac{\sum_i S_{CO2,i} V_i}{V} \qquad (3)$$

and

$$\overline{S}_{lr} = \frac{\sum_i MIN(S_{l,i}, S_{lr,i}) V_i}{V} \qquad (4)$$

In Eqs. 3 and 4, we consider the arbitrary storage volume to be divided into i discrete volumes as in typical numerical reservoir simulation methods. Furthermore, Eq. 4 accounts for effects of dry out near the well where S_l may become less than S_{lr} due to vaporization of H_2O into the CO_2 phase and is zero ($S_l = 0.0$) at full dry out. By this definition, $\overline{S}_{CO2}$ is the volumetrically weighted average CO_2 saturation (S_{CO2}) over the i volumes within the storage region defined by V where

$$V = \sum_i V_i = \phi \pi r^2 H \qquad (5)$$

and $\overline{S}_{lr}$ is the volumetrically weighted residual liquid (aqueous phase, or brine) saturation over the same cylindrical volume defined by the same r. By these definitions, RSE must always be specified along with the value of r used to define V through Eq. 5.

The advantage of defining the RSE as in Eq. 2 is that it accounts for spatially varying CO_2 saturations. Similarly, the spatial variation in residual liquid (native brine) saturation is taken into account in the definition of RSE where variations in S_{lr} can occur for many reasons arising from changes in rock properties (facies, texture, fractures, grain coatings, etc.) and/or in fluid properties (salinity, presence of hydrocarbon phases, etc.). Note that the pore volume taken up by salt precipitation that may accompany dry out in the near-well region [21, 22] is neglected in the present definition. In general, for typical choices of r, the volume of the near-well region where dry out and salt precipitation can occur will be a very small fraction of the overall volume occupied by CO_2.

The Case for Local Injection Control

Overcoming Variable Transmissivity

Injection wells are normally perforated using shaped charges that blast holes in the casing and cause local formation damage that enhances permeability in the near-well region along the injection interval. When an injection well is perforated uniformly, the entire perforated interval between packer and bottom cement, or within a packed-off interval, is effectively uniformly open to the formation. Other well completion approaches may be used, such as slotted liners, gravel packs, etc. For the purposes of this paper, it can be assumed that the resistance to fluid flow provided by well components is negligible relative to resistance provided by formation permeability. As such, bulk inflow out from the well at any level into the reservoir during injection is mostly controlled by the reservoir permeability-thickness product (transmissivity).

Flow is also controlled strongly by the lateral pressure gradient from well to formation. In most cases, the largest pressure gradient occurs at the first perforations (the shallowest in a vertical well, or nearest the heel in a horizontal well) that connect with a highly transmissive zone, leading to a large amount of flow occurring through these perforations [23]. Flow into the formation through deeper perforations still occurs, but the pressure-gradient driving force tends to be smaller because part of the pressure is reduced by flow into the first large-transmissivity zone(s) encountered by the injectate. Kumar and Bryant (2009) [24] proposed a simple model for specifying the length and locations of perforation intervals such that injection along the entire length of the interval will occur uniformly, even as reservoir pressure varies hydrostatically and there is dynamic injection pressure variation in the well. These authors further acknowledged that engineering the injection to cause uniform injection rate along the well might be associated with overall injectivity decline, but that the benefits of better reservoir sweep and smaller plume footprints could justify a decrease in injectivity [24].

The result of preferential injection into high-transmissivity zones as described above is illustrated in Figure 3(a) by a sketch of a non-specified well perforated across a vertically heterogeneous reservoir. The effective permeability (log scale) as estimated from a porosity log with averaging applied to approximate a series of layers is shown on the left-hand side. As shown by Figure

3(a), injected CO_2 tends to flow preferentially into the first transmissive layer leaving underutilized the low-transmissivity layers and to some extent both high- and low-transmissivity layers deeper in the well. Such an injection pattern is acceptable from the standpoint of injectivity alone, but it causes fast spreading of the free-phase CO_2 plume in the high-transmissivity layers, early breakthrough to potentially leaky surrounding wells, and overall inefficient CO_2 sweep and corresponding utilization of the entire pore space. This inefficient use of pore space starts in the near-well region, and then propagates to the reservoir scale.

Figure 3(b) shows a cartoon of CO_2 saturation in the same formation as in Figure 3(a) but for a case using unspecified local flow control methods that are capable of limiting flow in high-transmissivity layers and enhancing flow in low-transmissivity layers. As shown in Figure 3(b), local flow control methods allow CO_2 to be more uniformly injected into the formation leading to much more efficient utilization of pore space. Local flow control to enhance injection into low-transmissivity layers requires active control approaches such as those developed in the oil and gas industry in so-called intelligent completions [4]. A dual completion with two sets of tubing or other technology may be needed to achieve this kind of flow control where varying injection pressures may be needed to achieve desired injection rates. Note that preferential injection into initially low-transmissivity layers may be self-enhancing as dry out occurs faster for higher injection rates resulting in a lower-viscosity fluid ($scCO_2$) and higher CO_2 relative permeability. Regardless of whether self-enhancement occurs or not, the resulting more-efficient utilization of otherwise un-utilized storage pore space will propagate outward leading to smaller plume footprint size, which enables a smaller *r* to be used for averaging in RSE, ultimately leading to a larger value of RSE. This is true especially during the first several years of injection before the plume becomes dominated by buoyancy and/or high-permeability flow channels, if present, which control plume migration at later times. Injectivity (defined as the amount of CO_2 that can be injected per unit rise in local reservoir pressure) will be lower overall for the case shown in Figure 3b relative to 3a. Therefore, the advantages of better reservoir sweep and higher RSE would need to be weighed against the downside of higher costs and higher injection pressures that come with implementing local flow control technologies on a site-by-site basis, as decisions about injection design are being made. To be more specific, operators may compare pore space lease/acquisition costs against the costs of local flow control technology. It is notable that small reductions in the radius of roughly circular CO_2 free-phase plumes correspond to large incremental savings in per-acre land costs due to the quadratic dependence of land area on plume radius.

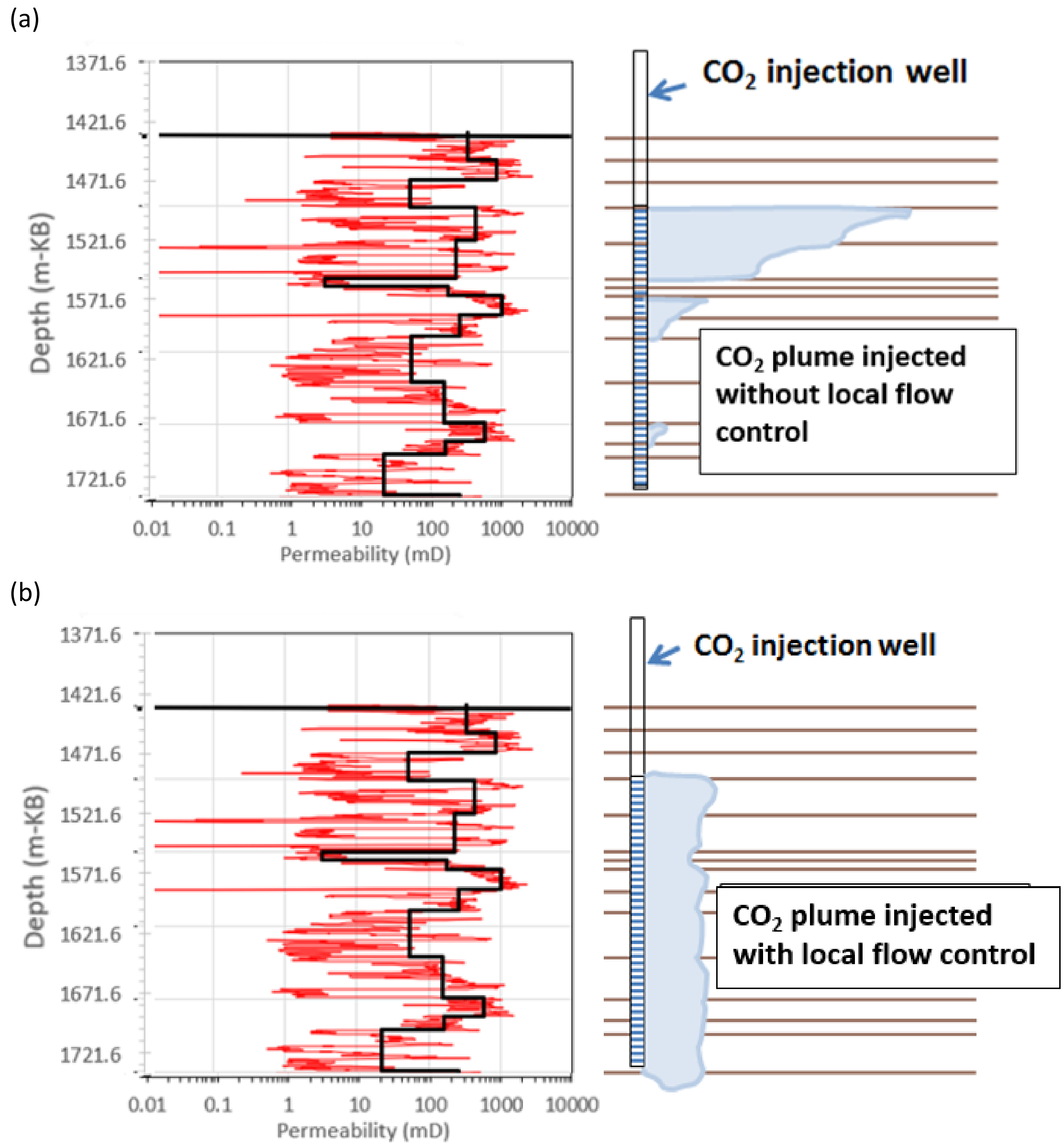

Figure 3. Permeability (red) (millidarcy) calculated from a porosity log versus depth below Kelly Bushing (m-KB) and averaged over layers to approximate horizontal permeability (black) (left-hand side) with sketch of a CO_2 injection well showing one slice of a radially symmetric CO_2 plume around the well (right-hand side). (a) Well without local flow control showing preferential flow caused by combination of high transmissivity in the formation and high lateral pressure gradients; (b) Relatively uniform phase-front advance achieved using local flow control devices.

Radial Storage Efficiency in Practice

Injection Design and Conformance Simulations

As with capacity and storage efficiency measures in general, RSE will find most of its use in modeling and simulation studies. This is because of the difficulty of making field measurements that quantify the terms in the RSE such as spatial distributions of CO_2 saturation and residual liquid saturation. While the dry-out region has been convincingly observed and monitored at the Ketzin test site [25], the state-of-the-art pulsed-neutron logging (PNL) approach relied upon to effectively monitor gas-phase saturation cannot detect dry regions (corresponding to free-phase CO_2) more than a few tenths of a meter from the tool into the formation. So, for the most part, measures of capacity and storage efficiency are mostly applicable and useful in modeling for injection design purposes.

Specifically, in the early stages of a project as the storage reservoir is being characterized and injection design carried out, coupled well-reservoir simulation using codes such as T2Well [26] can be used to estimate values of RSE for different injection designs with and without local flow control devices. Because of the large changes in pressure, temperature, and fluid property conditions in the near-well region, it is critically important to finely discretize (highly resolve) the numerical grid in the near-well region. Under-resolved flow models may run nicely but miss key processes of dry out, salt precipitation, decompression cooling, and phase change that occur over short length scales from the well through the perforations and into the near-well region of the storage reservoir.

Property boundaries and subsurface pore-space rights access will provide constraints on plume footprint size (values of r in RSE) at individual GCS sites within a basin. In early-stage studies at potential GCS sites, operators can use simulations to optimize injection design to match the project's surface property access rights taking advantage of the spatial variations inherent in CO_2 pore occupancy in the storage reservoir accounted for in the RSE equation. Similarly, later in the project development process, estimates of RSE and the associated r value may provide constraints on project pore-space acquisition costs. As an injection project moves into the operational stages with regular monitoring of free-phase CO_2 along the injection well or by means of PNL in nearby observation wells and/or by various geophysical approaches, RSE can be estimated from simulations constrained by monitoring data in the spirit of conformance modeling [27, 28]. Estimates of RSE may also be useful for guiding adjustments to tune local injection control devices to optimize RSE.

Example Simulations

To test and demonstrate local flow control and the use of RSE, simulations have been carried out of CO_2 injection into a hypothetical and idealized radially symmetric storage reservoir with four layers, with large permeability in the upper two layers, very low permeability in the third aquitard layer, and moderate permeability in the lowest layer. All of the layers except the aquitard have ten times higher horizontal permeability than vertical permeability ($k_v/k_h = 0.1$). Properties of the system are presented in Tables 1 and 2, and a sketch of the system is shown in Figure 4. Discretization of the 2D RZ domain into 2193 grid blocks (43 radial × 51 vertical) and the highly resolved near-well region (inset) are also shown in Figure 4.

Starting at the ground surface, the vertical well used in Case 1 (not shown fully in Figure 4) starts with a few wellhead grid blocks and then extends downward to the top of the reservoir in 25-m long grid blocks. From the top of the reservoir downward, the perforated well grid blocks match the thickness of the reservoir grid blocks one-for-one to the bottom of the reservoir totaling 129 grid blocks. Although the simulations were run non-isothermally, thermal effects do not play a significant role in the system and are not discussed here for the sake of brevity.

Two different injection scenarios were simulated: (Case 1) injection through a well equally perforated over all four layers, and (Case 2) injection through a virtual well with effectively two completions for implementing local flow control, one completion for injection into the upper high-permeability layers and the second for injection into the lower-most low-permeability layer. All of the 2D RZ simulations were carried out using T2Well/ECO2N [29, 26] with the objective of demonstrating how local flow control can be used to increase RSE when the storage reservoir is layered and some layers have lower permeability (or lower transmissivity).

Table 1. Properties of the tubing in the simplified model of the CO_2 injection well.

Tubing property	Value
Inner diameter	0.101 m over full vertical length of 2000 m
Roughness	55.1×10^{-6} m
Thermal conductivity	2.5 J s^{-1} K^{-1} m^{-1}
Heat capacity	1266 J kg^{-1} K^{-1}
Perforation area fraction (fraction of total surface area occupied by open holes)	0.20

Published in Greenhouse Gases: Science and Technology, 22 June 2021
https://doi.org/10.1002/ghg.2080

Table 2. 2D RZ reservoir properties.

Radially Symmetric Reservoir Properties	
Thickness	100 m
Depth of top of the reservoir	1900 m
Porosity (ϕ)	0.10
Permeability of the layers res01 (1900-1925 m) res02 (1925-1950 m) res03 (1950-1975 m) res04 (1975-2000 m)	k_R, k_Z 1×10^{-13}, 1×10^{-14} m^2 1×10^{-13}, 1×10^{-14} m^2 1×10^{-19}, 1×10^{-19} m^2 1×10^{-14}, 1×10^{-15} m^2
Compressibility	8.5×10^{-10} Pa^{-1}
Thermal conductivity	2.50 W/(m K)
Heat capacity (C_P)	1000 J/(kg K)
Capillary Pressure (P_{cap}) and Relative Permeability (k_r) *Terminology:* m = 1-1/n = power in expressions for P_{cap} and k_r S_{lr} = aqueous-phase residual saturation S_{gr}= gas-phase residual saturation P_{c0} = capillary pressure strength between aqueous and gas phases P_{cmax} = maximum possible value of P_{cap}	van Genuchten (1980) P_{cap} and k_r with Corey (1952) relative permeability for gas [30, 31] m = 0.50 S_{lr} = 0.37 for P_{cap}, 0.35 for k_r S_{gr} = 0.05 $P_{c0} = 1.25 \times 10^4$ Pa $P_{cmax} = 1 \times 10^7$ Pa
Initial pressure	Hydrostatic 18.8 MPa at top of reservoir 19.8 MPa at bottom of reservoir
Initial temperature	Geothermal gradient 18.2 °C/km Ground surface T = 11.0 °C 45.6 °C at top of reservoir 47.4 °C at bottom of reservoir
Initial saturation	Aqueous phase saturation (S_l) = 1.0
CO_2 injection rate	1 million tonnes per year (31.7 kg/s)

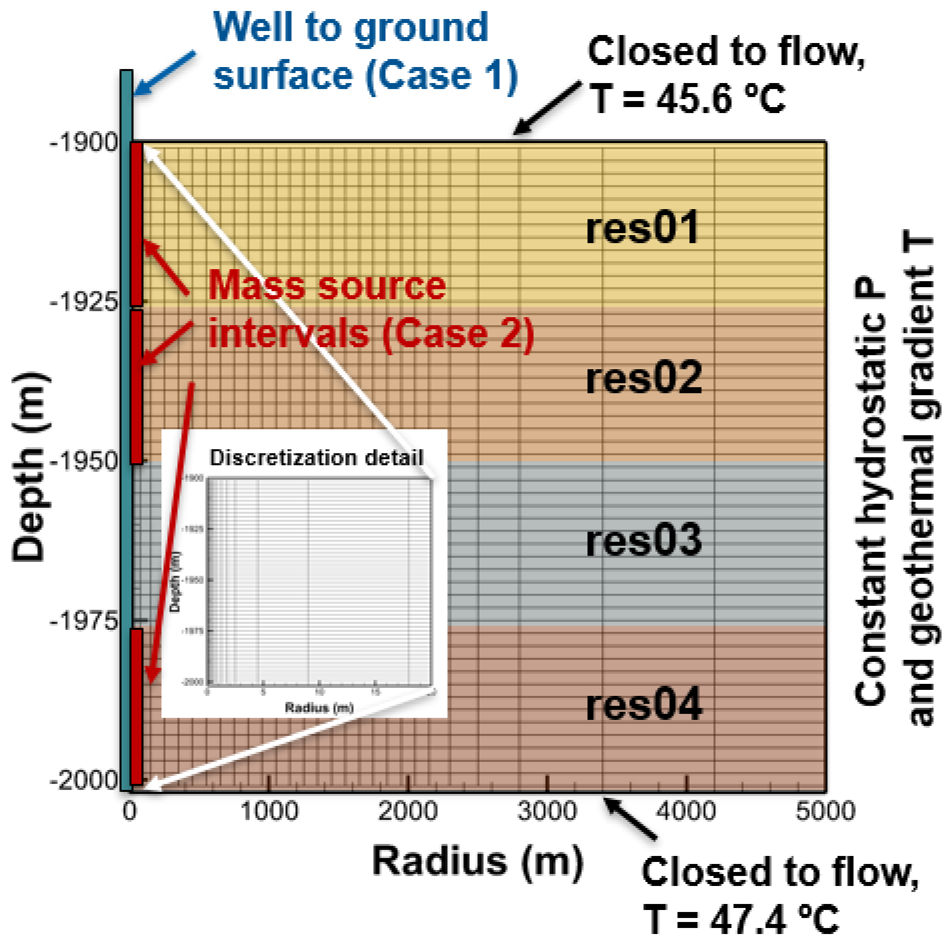

Figure 4. Hypothetical four-layer RZ reservoir model system with well (used in Case 1) shown on the left-hand side, mass source intervals (used in Case 2), boundary conditions on top, bottom and right-hand side, and discretization with inset showing details of the fine resolution around the well. The well extends to the ground surface and is perforated uniformly along the entire interval of the layered system. The mass sources in Case 2 specify injection into every grid block along the left-hand side of the domain in layers res01, res02, and res04 summing to 1 $MtCO_2$/yr. Note the large vertical exaggeration.

The simulation results of CO_2 injection for 20 years for Case 1, which specifies CO_2 injection at a rate of 1 million tonnes of CO_2 per year (31.7 kg/s) through a well with uniformly spaced perforations along the entire reservoir thickness, are shown in Figure 4a-b. Keeping in mind the geometry of the radial RZ system in which CO_2 saturations at larger radius represent much larger amounts of CO_2 than saturations at smaller radius, the figures show a negligible amount of CO_2 enters the aquitard layer (res03) and little CO_2 enters the lower low-permeability layer (res04). Also note that the dry-out region that occurs in res01 and res02 is much narrower in res04 and does not show up in the figure at the scale plotted. In short, the ten—times-lower permeability of the deepest layer (res04) inhibits injectivity there resulting in most of the CO_2 being injected into res01 and res02. This illustrates the challenge of efficiently using available pore space for CO_2 storage in heterogeneous reservoirs using standard injection wells without local flow control approaches.

In Case 2 shown in Figure 5c-d, injection was specified as a constant CO_2 mass generation rate with two-thirds of the total (21.1 kg/s) going into a virtual well perforated in the top two layers (res01 and res02), and one-third of the total (10.56 kg/s) going into a virtual well perforated in the bottom layer (res04). This is in contrast to Case 1 that employed a single well from the ground surface modeled as a coupled well-reservoir system using T2Well. By the method used in Case 2, the model system is roughly a dual-completion approach whereby a well would have two independent sets of tubing (with appropriate packers) set to deliver CO_2 independently to the layers in which the well is perforated. This approach would allow the operator to control the pressure (and flow rate) of each injection tubing system to account for higher and lower transmissivities of the target injection zones. As shown in Figure 5d, the simulation produces dry-out regions in all layers, and this injection approach causes a more efficient filling of all three permeable layers. Note that in both cases the injection rate is 1 million tonnes of CO_2 per year. The result of the lower transmissivity in res04 is a significantly higher pressurization in Case 2 as discussed further below.

https://doi.org/10.1002/ghg.2080

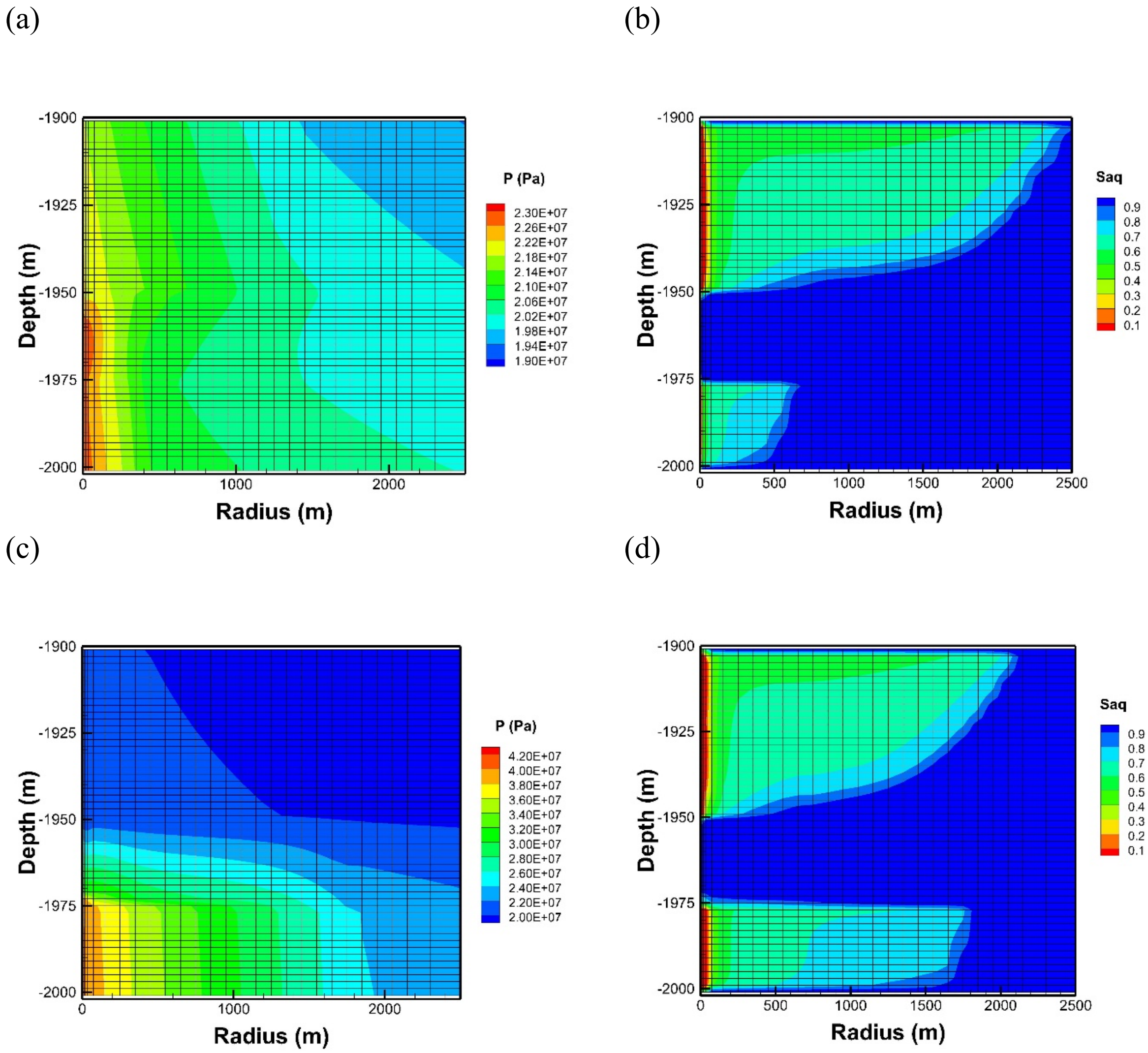

Figure 5. Simulation results after 20 years of injection showing pressure and aqueous phase saturation ($S_{aq} = S_l = 1 - S_{CO2}$) for Case 1 (a) and (b) and Case 2 (c) and (d). Note the lack of dry-out in the near-well region in the lower layer for Case 1 (b) and the higher injection pressure that resulted in the lower layer for Case 2 (note different scales of the pressure legends in (a) and (c)). Finally, note the maximum extent of the plume for Case 1 is approximately 2500 m while it is only 2200 m for Case 2 (see also Table 3).

In a post-processing step, values of RSE (Table 3) were calculated for Cases 1 and 2 by Eq. 2 for these results for various values of *r*. Note first in Table 3 that the total available pore volume for CO_2 storage accounting for the residual liquid saturation is the same for Cases 1 and 2. The volumetrically weighted average CO_2 saturation varies for the two cases and for various *r* values, but the RSE values show more and more agreement as *r* becomes larger and more of the injected CO_2 is included in the averaging. Four values of *r* were chosen: (1) 600 m, approximately the extent of the plume in the lowest layer (res04) in Case 1; (2) 1800 m, approximately the maximum extent of the plume in the lowest layer (res04) in Case 2; (3) 2200 m, approximately the maximum extent of the plume (occurs in layer res01) in Case 2, and (4) 2500 m, approximately the maximum extent of the plume (occurs in layer res01) in Case 1.

Results of RSE shown in Table 3 for these various *r* values show the sensitivity of RSE to *r*. Specifically, for *r* equal to approximately the radius (600 m) of the Case 1 plume in the lowest layer, RSE is 0.35 for Case 1 and 0.395 for Case 2 because saturations are higher in the lower layer in Case 2. For *r* equal to approximately the radius (1800 m) of the Case 2 plume in the deepest layer (res04), the RSE for Case 2 is 0.28 while it is only 0.23 for Case 1. The higher value of RSE in Case 2 is quantifying the effect of the increased amount of CO_2 within 1800 m of the well contributed by CO_2 the deepest layer (res04). In Case 1, this layer did not receive nearly as much CO_2 with injection through a simple well because the layer permeability (transmissivity) is ten times lower than in the two upper layers.

The effective dual completion modeled in Case 2 to force the lowest layer to receive CO_2 improved the RSE for $r = 1800$ m at the expense of higher injection pressure. Specifically, assuming the injection pressure in layer res04 was 40 MPa (5800 psi) and that this pressure was allowable because it was 90% of a hypothetical fracture pressure of 44 MPa (i.e., 90% of 44 Mpa (6700 psi) = 40 Mpa (5800 psi)), the frac gradient would be 22 kPa/m (0.97 psi/ft). This frac gradient is not unusual for sedimentary basins although some basins have smaller frac gradients and therefore an operator may have to reduce the lower-layer injection rate to comply with applicable frac-gradient requirements for injection into any specific reservoir.

As *r* increases from 600 m to 1800 m and 2500 m, the RSE values for Cases 1 and 2 become more equal because RSE becomes more like a conventional storage efficiency value averaging more and more of the injected CO_2 over more and more of the storage region. The Case 2 volumetrically weighted CO_2 saturation and RSE values are smaller than the Case 1 values because $r = 2500$ m is beyond the maximum extent of the Case 2 plume and therefore saturation is averaged over more volume not containing free-phase CO_2 making the volume averages decline.

Table 3. RSE and related properties calculated for the simulation results at t = 20 yrs shown in Figure 4..

RSE-related property	Case 1	Case 2	Case 1	Case 2	Case 1	Case 2	Case 1	Case 2
r (m)	600	600	1800	1800	2200	2200	2500	2500
Total formation volume within r (units of 10^9 m^3)	0.115	0.115	1.04	1.04	1.55	1.55	2.17	2.17
Volumetrically weighted $\overline{S}_{CO2}$	0.227	0.257	0.147	0.181	0.127	0.130	0.0958	0.0929
RSE	0.349	0.395	0.227	0.279	0.196	0.200	0.147	0.143

For an actual GCS storage complex, there may be many hydraulically distinguishable layers with variable transmissivity and operators may have a limited number of storage zones that they can practically treat using local flow control approaches in any given well. On the other hand, there may be also multiple approaches for effective local flow control which could lead to more of the layers being practically addressed. For example, in addition to the multiple completion approach illustrated above, it is possible that a simple varying of perforation density longitudinally along the well and/or other valving approaches could be used to effect flow control depending on the transmissivity contrasts and storage opportunities presented by each layer.

Conclusions

RSE is an extension of existing measures of storage efficiency that emphasizes maximizing injection and storage throughout the vertical extent of the storage region along a vertical well to minimize the footprint of the CO_2 saturation plume. Without local flow control e.g., as controlled by intelligent well completions, varying transmissivity in layers across the vertical extent of a storage complex leads to inefficient use of available pore space. To address this problem, operators and reservoir engineers can utilize existing oil and gas intelligent well technology for flow control or develop new approaches tailored for CO_2 injection and trapping and capable of compensating for low- and high-transmissivity layers/zones in the storage region. The concept of RSE for quantifying the effectiveness of local flow control can be used in injection design simulations. Improving the uniformity of free-phase CO_2 sweep in a heterogeneous sedimentary reservoir using local flow control methods inherently involves locally higher injection pressures. Implementing local flow control methods is mostly relevant during the early phases of a GCS project when the CO_2 free-phase plume footprint size is important, and this approach will become less important late in projects when reservoir/basin pressure becomes the limiting factor on capacity. Local flow control and RSE are applicable to both vertical and horizontal wells, although the objective of minimizing plume footprint does not translate directly from vertical to horizontal wells.

Acknowledgment

Thanks to Christine Doughty (LBNL) for review and discussion of an earlier draft. Useful revisions to the draft manuscript were prompted by the constructive review comments of Philip Ringrose (Equinor) and an anonymous reviewer. This work was supported by TOTAL E&P Recherche and Developpement and by Lawrence Berkeley National Laboratory under Department of Energy Contract No. DE-AC02-05CH11231.

References

1. Zhou, Q. and Birkholzer, J.T., 2011. On scale and magnitude of pressure build-up induced by large-scale geologic storage of CO_2. Greenhouse Gases: Science and Technology, 1(1), pp.11-20.

2. Thibeau, S., Mucha, V., 2011. Have we overestimated saline aquifer CO_2 storage capacities? Oil Gas Sci. Technol. Rev. IFP Energies nouvelles 66 (1), 81–92.

3. Birkholzer, J.T., Oldenburg, C., Zhou, Q., 2015. CO_2 migration and pressure evolution in deep saline aquifers. Int. J. Greenh. Gas Control 40, 203–220.

4. Joubran, J., 2018, April. Intelligent Completions: Design and Reliability of Interval Control Valves in the Past, Present, and Future. In Offshore Technology Conference. Offshore Technology Conference.

5. Brnak, J.J., Petrich, B. and Konopczynski, M.R., 2006, January. Application of SmartWell technology to the SACROC CO_2 EOR project: A case study. In SPE/DOE Symposium on Improved Oil Recovery. Society of Petroleum Engineers.

6. Buscheck, T.A., Sun, Y., Chen, M., Hao, Y., Wolery, T.J., Bourcier, W.L., Court, B., Celia, M.A., Friedmann, S.J. and Aines, R.D., 2012. Active CO_2 reservoir management for carbon storage: Analysis of operational strategies to relieve pressure buildup and improve injectivity. International Journal of Greenhouse Gas Control, 6, pp.230-245.

7. Kopp, A., Class, H., Helmig, R., 2009a. Investigations of CO_2 storage capacity in deep saline aquifers. Part 1. Dimensional analysis of flow processes and reservoir characteristics. Int. J. Greenh. Gas Control 3 (3), 263–276.

8. Bachu, S., 2015. Review of CO_2 storage efficiency in deep saline aquifers. International Journal of Greenhouse Gas Control, 40, pp.188-202.

9. van der Meer, L.G.H., 1995. The CO_2 storage efficiency of aquifers. Energy conversion and management, 36(6-9), pp.513-518.

10. Doughty, C., Pruess, K., Benson, S.M., Hovorka, S.D., Knox, P.R. and Green, C.T., 2001. Capacity investigation of brine-bearing sands of the Frio Formation for geologic sequestration of CO_2. GCCC Texts and Reports.

11. Bachu, S., Bonijoly, D., Bradshaw, J., Burruss, R., Holloway, S., Christensen, N.P. and Mathiassen, O.M., 2007. CO_2 storage capacity estimation: Methodology and gaps. International journal of greenhouse gas control, 1(4), pp.430-443.

12. Nordbotten, J.M., Celia, M.A. and Bachu, S., 2005. Injection and storage of CO 2 in deep saline aquifers: analytical solution for CO 2 plume evolution during injection. Transport in Porous media, 58(3), pp.339-360.

13. Okwen, R.T., Stewart, M.T. and Cunningham, J.A., 2010. Analytical solution for estimating storage efficiency of geologic sequestration of CO_2. International Journal of Greenhouse Gas Control, 4(1), pp.102-107.

14. Ringrose, P., 2020. Geological storage of CO2: processes, capacity and constraints. In *How to Store CO2 Underground: Insights from early-mover CCS Projects* (pp. 13-83). Springer, Cham.

15. Kopp, A., Class, H., Helmig, R., 2009b. Investigations of CO_2 storage capacity in deep saline aquifers. Part 2. Estimation of storage capacity coefficients. Int. J. Greenh. Gas Control 3 (3), 277–287.

16. Brennan, S.T., Burruss, R.C., Merrill, M.D., Freeman, P.A. and Ruppert, L.F., 2010. A probabilistic assessment methodology for the evaluation of geologic carbon dioxide storage. US Geological Survey Open-File Report, 1127(2010), p.31.

17. Ringrose, P.S., 2018. The CCS hub in Norway: some insights from 22 years of saline aquifer storage. Energy Procedia, 146, pp.166-172.

18. Doughty, C., S.M. Benson, K. Pruess, Capacity Investigation of Brine-Bearing Sands for Geologic Sequestration of CO_2, Greenhouse Gas Control Technologies, 6, II, 1645-1648, 2003.

19. Kumar, N. and Bryant, S., 2008, January. Optimizing injection intervals in vertical and horizontal wells for CO_2 sequestration. In SPE Annual Technical Conference and Exhibition. Society of Petroleum Engineers.

20. Oldenburg, C.M., Mukhopadhyay, S. and Cihan, A., 2016. On the use of Darcy's law and invasion-percolation approaches for modeling large-scale geologic carbon sequestration. Greenhouse Gases: Science and Technology, 6(1), pp.19-33.

21. Pruess, K. and Müller, N., 2009. Formation dry-out from CO_2 injection into saline aquifers: 1. Effects of solids precipitation and their mitigation. Water Resources Research, 45(3).

22. Piao, J., Han, W.S., Choung, S. and Kim, K.Y., 2018. Dynamic Behavior of CO_2 in a Wellbore and Storage Formation: Wellbore-Coupled and Salt-Precipitation Processes during Geologic CO_2 Sequestration. Geofluids, 2018.

23. Vilarrasa, V., Carrera, J., Bolster, D. and Dentz, M., 2013. Semi analytical Solution for CO_2 Plume Shape and Pressure Evolution During CO_2 Injection in Deep Saline Formations. Transport in porous media, 97(1), pp.43-65.

24. Kumar, N. and Bryant, S.L., 2009. Semi-analytical model to determine perforation interval for secure CO_2 storage in saline aquifers. Energy Procedia, 1(1), pp.3071-3078.

25. Baumann, G., Henninges, J., De Lucia, M., 2014. Monitoring of saturation changes and salt precipitation during CO_2 injection using pulsed neutron-gamma logging at the Ketzin pilot site. Int. J. Greenh. Gas Control 28, 134–146.

26. Pan, L. and Oldenburg, C.M., 2014. T2Well—an integrated wellbore–reservoir simulator. Computers & Geosciences, 65, pp.46-55.

27. Chadwick, R.A. and Noy, D.J., 2015. Underground CO_2 storage: demonstrating regulatory conformance by convergence of history-matched modeled and observed CO_2 plume behavior using Sleipner time-lapse seismics. Greenhouse Gases: Science and Technology, 5(3), pp.305-322.

28. Oldenburg, C.M., 2018. Are we all in concordance with the meaning of the word conformance, and is our definition in conformity with standard definitions?. Greenhouse Gases: Science and Technology, 8(2), pp.210-214.

29. Pan, L., Oldenburg, C.M., Pruess, K. and Wu, Y.S., 2011. Transient CO2 leakage and injection in wellbore-reservoir systems for geologic carbon sequestration. *Greenhouse Gases: Science and Technology*, *1*(4), pp.335-350.

30. van Genuchten, M.T., 1980. A closed-form equation for predicting the hydraulic conductivity of unsaturated soils 1. Soil science society of America journal, 44(5), pp.892-898.

31. Corey, A.T., 1954. The interrelation between gas and oil relative permeabilities. Producers monthly, 19(1), pp.38-41.